

OPEN

Detection of Gram-negative bacterial outer membrane vesicles using DNA aptamers

Hye-Su Shin, Vinayakumar Gedi, Joon-Ki Kim & Dong-ki Lee

Infection of various pathogenic bacteria causes severe illness to human beings. Despite the research advances, current identification tools still exhibit limitations in detecting Gram-negative bacteria with high accuracy. In this study, we isolated single-stranded DNA aptamers against multiple Gram-negative bacterial species using Toggle-cell-SELEX (systemic evolution of ligands by exponential enrichment) and constructed an aptamer-based detection tool towards bacterial secretory cargo released from outer membranes of Gram-negative bacteria. Three Gram-negative bacteria, *Escherichia coli* DH5 α , *E. coli* K12, and *Serratia marcescens*, were sequentially incubated with the pool of random DNA sequences at each SELEX loop. Two aptamers selected, GN6 and GN12, were 4.2-times and 3.6-times higher binding to 10⁸ cells of Gram-negative bacteria than to Gram-positive bacteria tested, respectively. Using GN6 aptamer, we constructed an Enzyme-linked aptamer assay (ELAA) to detect bacterial outer membrane vesicles (OMVs) of Gram-negative bacteria, which contain several outer membrane proteins with potent immunostimulatory effects. The GN6-ELAA showed high sensitivity to detect as low as 25 ng/mL bacterial OMVs. Aptamers developed in this study show a great potential to facilitate medical diagnosis and early detection of bacterial terrorism, based on the ability to detect bacterial OMVs of multiple Gram-negative bacteria.

Bacterial infections can be detrimental due to their virulence factors, underscoring the need for development of rapid, accurate, and sensitive detection techniques¹. Gram-negative bacteria especially represent an important medical challenge. They are resistant to various antibiotics because their outer membrane evolves and adapts to the protective mechanisms against the selection pressure of antibiotics². Lipopolysaccharides (LPS), a major constituent of the outer membrane of Gram-negative bacteria, induces a strong innate immune response in host environments³. Furthermore, outer membrane vesicles (OMVs) with size of 20 to 250 nm, which are commonly produced and secreted from outer membranes of bacteria, carry various bacterial membrane proteins and other virulence factors^{4,5}. OMVs are known to trigger severe pathogenesis, enhance bacterial survival, transfer genetic and protein components for cell-free intercellular communication, deliver toxic compounds, and trigger immune response in host cells^{6,7}.

Various surface antigens exist on the cell surface of Gram-negative bacteria, which can be potential targets for bacterial detection. These antigenic moieties, including LPS^{8,9}, peptidoglycans^{10,11} and lectins¹² have served as substrates of the bioreceptors. Conventional methods of bacterial detections in general rely upon three types of laboratory-based techniques such as optical assays using fluorescent labeling^{13,14} or surface plasmon resonance¹⁵, mechanical quartz crystal microbalance sensors^{16,17} and electrochemical sensors¹⁸ such as potentiometric, amperometric and impedimetric assays. Despite the vast amount of research, sensitive bacterial detection methods which meet commercial demands in real situations are yet to be developed¹⁹. Detecting living bacteria in blood is difficult due to the immune regulation of host cells and the serum bactericidal activity^{20,21}. This suggests that the detection of bacterial OMVs is more effective than the detection of bacterial cells in clinical blood samples²².

In this study, nucleic acid aptamers are proposed for the development of inexpensive and rapid diagnostic tools, because aptamers could recognize target epitopes with high selectivity and specificity using the screening technique of systemic evolution of ligands by exponential enrichment (SELEX)²³. Using cell-SELEX, aptamers can be isolated against target epitopes in its natural physiological context, even when the exact target on the cell surface is unknown^{24,25}. Using bacterial cell-SELEX, several aptamers have been isolated against different bacterial

Department of Chemistry, Sungkyunkwan University, Suwon, 16419, Korea. Correspondence and requests for materials should be addressed to D.-k.L. (email: dklee0318@gmail.com)

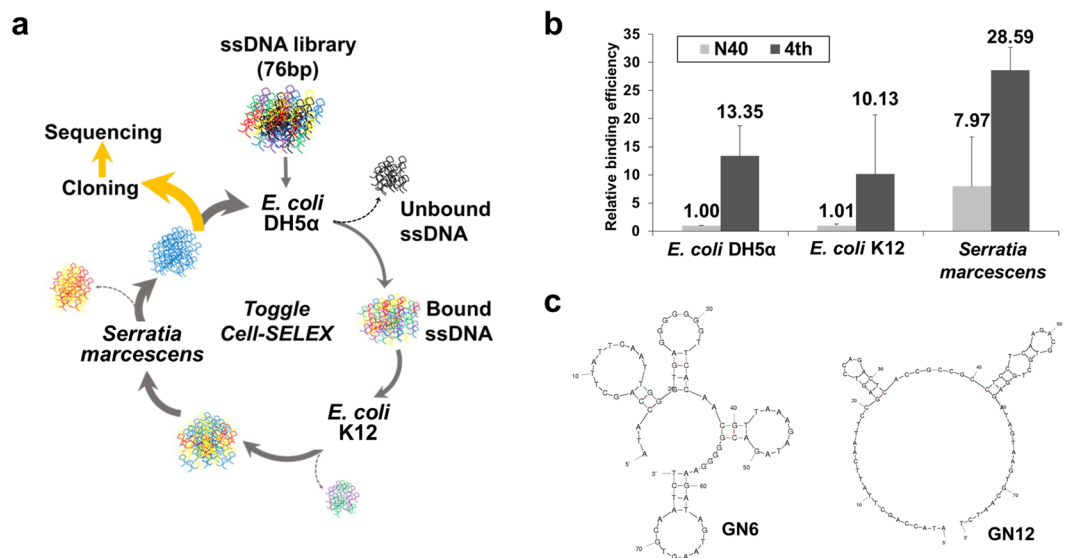


Figure 1. Toggle-Cell SELEX against multiple Gram-negative bacteria. (a) Schematic illustration of Toggle-Cell SELEX against three different Gram-negative bacteria. (b) Relative binding efficiency was tested using qPCR to confirm the enrichment of ssDNA after 4th round of Toggle SELEX. Data represented mean \pm SD values of three independent experiments. (c) Predicted secondary structures of two isolated aptamers, GN6 and GN12, using M-fold algorithm at 25 °C, $[\text{Na}^+] = 100 \text{ mM}$, and $[\text{Mg}^{2+}] = 5 \text{ mM}$.

species with high affinity and specificity. The dissociation constants (K_d) of several reported aptamers are in the nanomolar range with low limit of detection of about 1 to 1000 CFU/mL²⁶.

Although most bacterial cell-SELEX studies focus on targeting single bacterial strain, it is possible that aptamers could bind epitopes commonly shared among different bacterial strains^{27,28}. A previous study which performed SELEX against a single *E. coli* strain demonstrated that the selected aptamers can also bind other strains of *E. coli*, implicating that some bacterial strains share common targets on their cell surface²⁹. It also means that toggling different targets of interest beyond the conventional SELEX procedure can isolate cross-reactive aptamers with broad range of binding^{30,31}. One recent study reported isolation of aptamers against six different genera of bacteria using Toggle-cell SELEX³².

Here, we used Toggle-cell SELEX to generate single stranded DNA aptamers which exhibit broad cross-reactivity to different Gram-negative bacterial strains. Three bacteria in Enterobacteriaceae, *Escherichia coli* DH5 α , *Escherichia coli* K12, and *Serratia marcescens* were selected in the screening. After four rounds of toggle loops, the selected aptamers were characterized. Two selected aptamers, GN6 and GN12, showed broad binding efficiency to multiple strains of Gram-negative bacteria, but not to Gram-positive bacteria. Using GN6 aptamer, we constructed an Enzyme-linked aptamer assay (ELAA)^{33,34} to detect outer membrane vesicles (OMVs) of Gram-negative bacteria, which contain several outer membrane proteins with potent immunostimulatory effects. This GN6-ELAA platform showed high sensitivity to detect as low as 25 ng/mL bacterial OMVs.

Results and Discussion

Gram-negative bacterial Toggle-cell SELEX. Bacterial Toggle-cell SELEX was performed to isolate ssDNA aptamers against multiple Gram-negative bacteria. Three Gram-negative bacteria, *E. coli* DH5 α , *E. coli* K12, and *S. marcescens*, were selected for the isolation of aptamers (Fig. 1a). In the first round of selection, *E. coli* DH5 α cells were incubated with the random 76-nt ssDNA library. Unbound ssDNA mixture was discarded, and only bound ssDNA pool was recovered and amplified by PCR for next enrichment. Next, *E. coli* K12 and *S. marcescens* were used sequentially in the same procedures. This toggle loop was repeated 4 times until the relative amount of binding, measured using quantitative real-time PCR, of DNA aptamers mixtures was 13.35-, 10.03- and 3.59- times higher than that of the starting DNA library to three bacteria, respectively (Fig. 1b). The final products were amplified and cloned for sequencing analysis. After selection of two DNA sequences, GN6 and GN12, as aptamer candidates (Table 1), their secondary structures were predicted at 25 °C in buffer solutions which contain 5 mM MgCl_2 , 100 mM NaCl using M-fold algorithm (Fig. 1c).

Binding affinity of isolated aptamers. Next, we quantified binding affinities of GN6 and GN12 aptamers against three Gram-negative bacteria used in SELEX. Various concentrations of aptamers labelled with FAM (carboxyfluorescein) at the 3'-end were added to 10^8 cells of bacteria. After measuring the fluorescence signal, the binding saturation curves were fitted using non-linear regression model, based on the following equation: $S = B_{max} \times C / (K_d + C)$ (where S represents the fluorescence (FAM) intensity, B_{max} the maximum binding intensity, K_d the dissociation constant, and C, concentrations of aptamer) (Fig. 2a-c). The dissociation constants (K_d) were observed in the range of 20.36 to 59.70 nM against three bacterial strains tested (Table 2). These values were in similar range with previous experimental results in other studies²⁶. The binding affinities of two aptamers were compared with that of random ssDNA (N40) at 250 nM concentration in 10^8 and 10^5 cells of Gram-negative

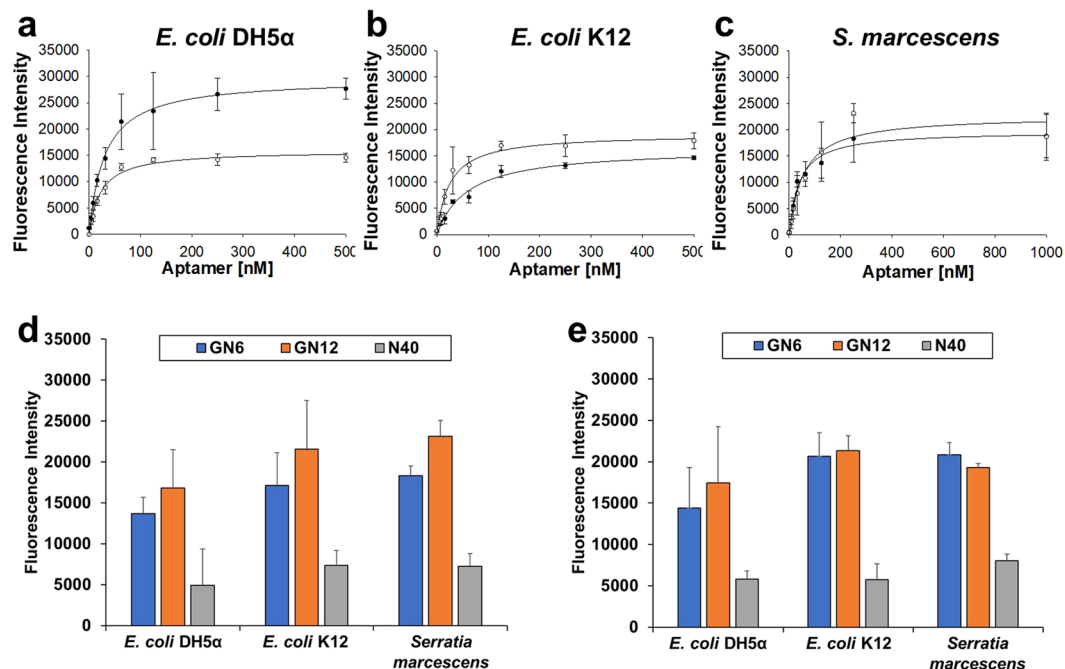


Figure 2. Binding affinity of GN6 and GN12 to three Gram-negative bacteria. Binding saturation curves of both GN6 (●) and GN12 (○) were fitted using non-linear regression model of SigmaPlot 12.0 towards (a) *E. coli* DH5α, (b) *E. coli* K12 and (c) *S. marcescens*. (d) 10⁸ cells and (e) 10⁵ cells of bacteria were incubated with the two selected aptamers at 250 nM concentration and N40 library as control. Data represents mean ± SD values of three independent experiments.

ID	DNA sequence (5' to 3')
GN6	ATA CCA GCT TAT TCA ATT GGG TGA GGG GGG GTT CAC AAC GTT AAA GAT AGA CGG GGG AAG ATA GTA AGT GCA ATC T
GN12	ATA CCA GCT TAT TCA ATT CCG AGT CCA GAC TCA CCG CCG CCT CCT CAA GAC GTG CTG GAG ATA GTA AGT GCA ATC T

Table 1. ssDNA sequences of two isolated aptamers after Gram-negative bacterial Toggle-cell SELEX.

Aptamer	<i>E. coli</i> DH5α	<i>E. coli</i> K12	<i>S. marcescens</i>
GN6	29.94 ± 2.49 nM	59.70 ± 10.89 nM	38.98 ± 6.46 nM
GN12	20.36 ± 2.38 nM	24.80 ± 3.98 nM	53.83 ± 17.70 nM

Table 2. Dissociation constants (K_d) of GN6 and GN12 aptamers against three bacteria.

bacteria, respectively (Fig. 2d,e). Both GN6 and GN12 aptamers showed average 2.55- and 3.19-times higher binding towards 10⁸ cells of bacteria than N40 random sequence. Likewise, it showed average 2.89- and 3.03-times higher binding to 10⁵ cells of bacteria than the same control.

Aptamer cross-reactivity towards multiple Gram-negative bacteria. Next, the broad cross-reactivity of selected aptamers was analysed by performing binding assay against multiple Gram-negative bacteria, based on the assumption that they share similar structural binding components as common cell surface epitopes. Both GN6 and GN12 (250 nM) showed high binding to 10⁸ cells of various Gram-negative bacteria tested, including the well-known pathogenic species, *K. pneumoniae*, *E. cloacae* and *S. sonnei* (Fig. 3a). It should be noted that aptamers showed lower binding to one Gram-negative bacteria tested, *S. trueperi*, which is a *Sphingomonas* species that belongs to α-proteobacteria³⁵. In contrast, significantly reduced binding efficiency was observed against all Gram-positive bacterial strains tested. GN6 aptamer could detect Gram-negative bacteria 4.2-times higher than Gram-positive bacteria ($p < 0.0001$). GN12 aptamer also showed 3.6-times higher binding to Gram-negative bacteria than Gram-positive bacteria ($p < 0.0005$) (Fig. 3b). These broad cross-reactivity and specificity to Gram-negative bacteria were also observed when 10⁵ cells of bacteria were incubated (Fig. S1a). Both GN6 and GN12 aptamer at 250 nM concentration were able to detect Gram-negative bacteria 3.9-times and 3.4-times higher than Gram-positive bacteria, respectively ($p < 0.0001$) (Fig. S1b). Without negative selections against Gram-positive bacteria during Toggle-cell SELEX, selected aptamers showed no binding preference to them, suggesting that the unknown targets of aptamers on cell surface exclusively expressed in Gram-negative bacteria.

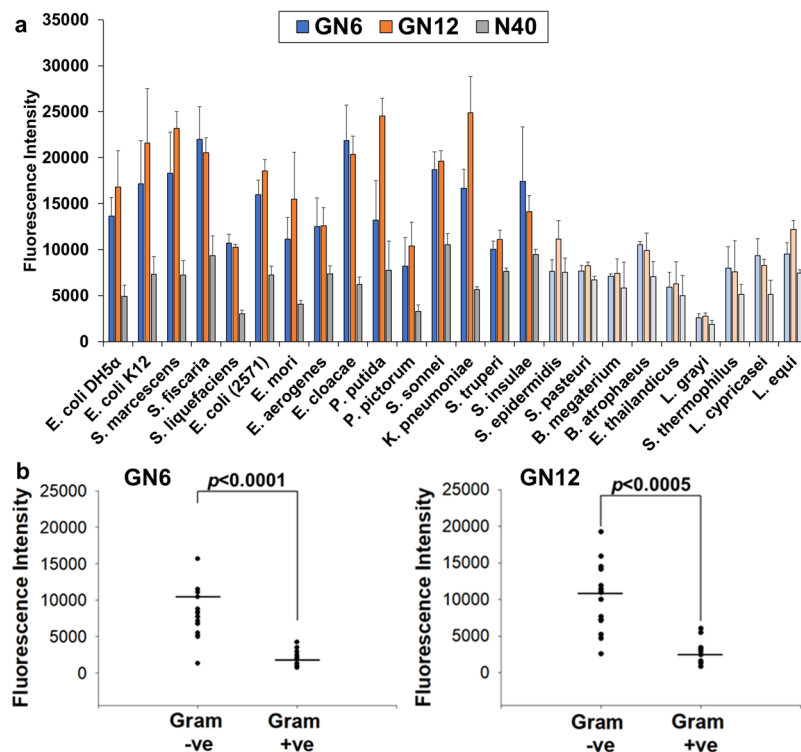


Figure 3. Binding profile of GN6 and GN12 against Gram-negative and positive bacteria. (a) Binding assay was performed using GN6 (blue) and GN12 (orange) at 250 nM against 10^8 cells of multiple Gram-negative (vivid) and Gram-positive (pale) bacteria. Binding efficiencies were estimated by measuring the fluorescence intensity of bound aptamers to bacteria. (b) GN6 (left) and GN12 (right) showed 4.2-times and 3.6-times higher binding to 10^8 cells of Gram-negative bacteria than to Gram-positive bacteria tested, respectively. Data represented mean \pm SD values of three independent experiments and p -values were analyzed using student's t -test.

	Z-average (diameter, nm)	PDI (Polydispersity index)
<i>E. coli</i> DH5 α	105.9	0.455
<i>E. coli</i> K12	97.96	0.420
<i>S. marcescens</i>	164.4	0.335
<i>L. grayi</i>	176.4	0.490
<i>B. megaterium</i>	84.29	0.410

Table 3. Size evaluations of bacterial OMVs via DLS.

Future studies are required to identify the specific targets of GN6 aptamers on OMVs surface. Furthermore, we also noticed inconsistency between dissociation constants and binding profiles of both aptamers regarding their binding abilities to Gram-negative bacteria. Higher binding affinity of aptamers with low K_d values generally represents the higher intermolecular interaction between a single target on bacteria and its bound aptamer. In contrast, Fig. 3 showed the maximum binding capacity (B_{max}) when all targets are fully saturated by excessive amounts of aptamers (250 nM). These two binding parameters, affinity and capacity, can be separately interpreted because capacity is affected by several factors such as multivalent interactions when an aptamer shares multiple antigens of bacteria or the density of targets on bacterial outer membrane^{29,36}.

Isolation and characterizations of bacterial OMVs. It has been known that OMVs budding out from outer membranes of Gram-negative bacteria carry several virulence biomolecules and endotoxins⁷. We isolated bacterial OMVs using ultracentrifugation. DLS analysis exhibited the size distribution of OMVs ranging from 84.29 to 176.4 nm (Table 3), within the range of general agreement^{4,5}. There are no general bacterial OMV markers, but OMV proteins such as OmpA (35.2 kDa) in *E. coli*³⁷ and Serralysin (~52–55 kDa) in *S. marcescens*³⁸ could be used for characterization (Fig. S2). Next, magnetic bead-pull down assay using streptavidin-coated beads and 3'-biotinylated GN6 aptamer was performed to capture OMVs³⁹ (Fig. 4a). The binding between *E. coli* DH5 α OMVs and GN6 was visualized by scanning electron microscope (SEM) (Fig. 4b). Without GN6 aptamer, spherical nanoparticles of *E. coli* DH5 α OMVs were not shown. It suggests that the targets of GN6 on *E. coli* DH5 α are

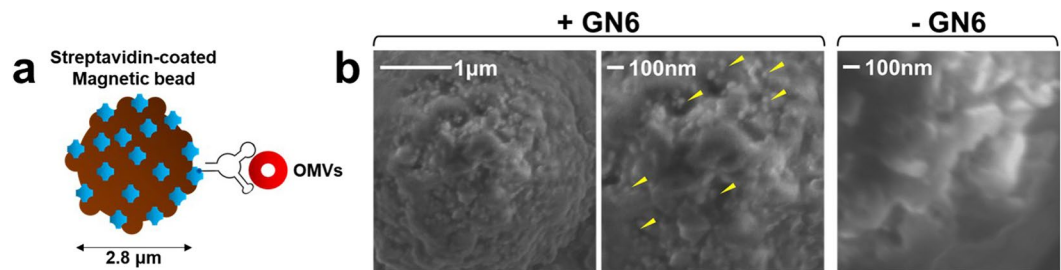


Figure 4. *E. coli* DH5 α -derived OMVs bound to GN6 aptamer. (a) Scheme of Bead-GN6-*E. coli* DH5 α OMVs complex. (b) SEM images of *E. coli* DH5 α -derived OMVs (yellow arrow) bound to GN6 aptamer. Without GN6 aptamer, no OMVs were shown.

also present in *E. coli* DH5 α OMVs. This leads us to develop an aptamer-based detection platform for bacterial OMVs.

ELAA platform for detecting Gram-negative bacterial OMVs. Using the selected aptamer, GN6, we have developed an Enzyme-linked aptamer assay (ELAA) to detect OMVs originated from various Gram-negative bacteria. Instead of conventional ELISA using the detection antibody conjugated with HRP (Horse radish peroxidase), GN6 aptamer was used as a bait (Fig. 5a). GN6 ELAA showed highly recognizable signals against three Gram-negative bacterial OMVs. The dissociation constants of GN6 to OMVs derived from *E. coli* DH5 α , *E. coli* K12 and *S. marcescens* were $0.13 \pm 0.01 \mu\text{g/ml}$, $3.70 \pm 0.98 \mu\text{g/ml}$ and $0.23 \pm 0.16 \mu\text{g/ml}$, respectively ($R^2 = 0.99$) (Fig. 5b). It especially showed the highest binding affinity and capacity to *E. coli* DH5 α OMVs. Meanwhile, this assay also showed high sensitivity, which could detect as low as 25 ng/mL of Gram-negative bacterial OMVs. Consistent with GN6 binding affinity to bacterial cells, it showed the similar pattern to binding affinity to bacterial OMVs, strongly suggesting that target of GN6 aptamers is present both on Gram-negative bacterial cells and on the surface of Gram-negative bacterial OMVs. Consistent with the previous results, OMVs from Gram-positive bacteria, *L. grayi* and *B. megaterium*, showed no recognizable binding to GN6 (Fig. 5c,d). These results indicate that GN6 ELAA could detect multiple Gram-negative bacteria derived OMVs. It opens the new possibility of developing cell-free bacterial sensor using bacterial OMVs as substrates instead of living bacterial cells.

Conclusion

While various systems are being developed to detect pathogenic bacteria, few studies have reported the isolation of broadly cross-reactive aptamers against various species of bacteria. Here, we developed highly specific DNA aptamers, GN6 and GN12, against many Gram-negative bacteria, including pathogenic strains. Selected aptamers after Toggle-cell SELEX showed broad cross-reactivity towards many Gram-negative bacteria tested. Using GN6 aptamer, we developed an GN6-ELAA to detect Gram-negative bacterial OMVs from cell-free supernatant. This is because unknown targets of GN6 on the original bacterial outer membrane could also be expressed in the surface of bacterial OMVs. Moreover, the GN6-ELAA had high sensitivity to low concentration of Gram-negative bacterial OMVs and high specificity exclusively bound to them. Further studies will require identification of GN6 aptamer targets and increasing the yield and purity of OMVs. If we increase the final yield and purity of OMVs, it will be possible that the detection of bacterial OMVs in cell-free medium leads to the accurate identification of the originated bacteria. We believe that the aptamer-based Gram-negative bacterial OMV detection has a great potential to facilitate medical diagnosis and early detection of bacterial terrorism.

Methods

Bacterial strains and culture. All bacteria were purchased from the Korean Collection for Type Culture (KCTC, Korea). *E. coli* DH5 α , *E. coli* K12, *E. coli* (KCTC 2571), *S. sonnei*, *K. pneumoniae*, *S. epidermidis* and *S. pasteurii* were cultivated at 37 °C in LB medium, *S. marcescens*, *S. ficaria*, *S. liquefaciens*, *E. mori*, *E. aerogenes*, *E. cloacae*, *B. megaterium*, and *B. atrophaeus* were grown at 30 °C in NB medium, *P. putida*, *P. pictorum*, and *S. insulae* were grown at 25 °C in LB medium, *E. thailandicus*, *S. thermophilus*, *L. cypricasei*, and *L. equi* were grown at 37 °C in Lactobacillus MRS broth, and *L. grayi* at 37 °C in BHI medium. All these bacteria were cultured under aerobic conditions up to OD₆₀₀ of 0.4, followed by centrifugation (10,000 rpm) for 10 min at 4 °C, and washing twice with Tris-HCl buffer (50 mM Tris, pH 7.4, 1 mM MgCl₂, 5 mM KCl, 100 mM NaCl). The washed bacteria were resuspended in binding buffer (50 mM Tris, pH 7.4, 5 mM MgCl₂, 5 mM KCl, 100 mM NaCl, 1 mg/mL BSA, 0.1 mg/mL Salmon sperm DNA, 0.1 mg/mL yeast tRNA).

Gram negative bacterial Toggle-Cell SELEX. All oligonucleotides were purchased from Integrated DNA technologies (Coralville, USA). The PAGE-purified single-stranded DNA library consisted of an N₄₀ randomized region flanked by two 18-nt primer-binding regions for PCR (5'-ATA CCA GCT TAT TCA ATT-N₄₀-AGA TAG TAA GTG CAA TCT-3'). The following forward primer (5'-ATA CCA GCT TAT TCA ATT-3) and reverse primer (5'-AGA TTG CAC TTA CTA TCT-3') were used for quantitative real-time PCR. The reverse primer modified with poly-A tail overhang (5'-AAA AAA AAAAAAAAAAAAAA AA/iSp9//iSp9/AGA TTG CAC TTA CTA TCT-3') was used for PCR in SELEX process. In the first round of SELEX, the ssDNA library pool (2500 pmol) was denatured in binding buffer for 5 min at 95 °C and cooled on ice for 5 min. It was mixed with 10⁸ number of *E. coli* DH5 α cells in binding buffer with constant shaking at RT for 15 min. The ssDNA bound to *E. coli* DH5 α was

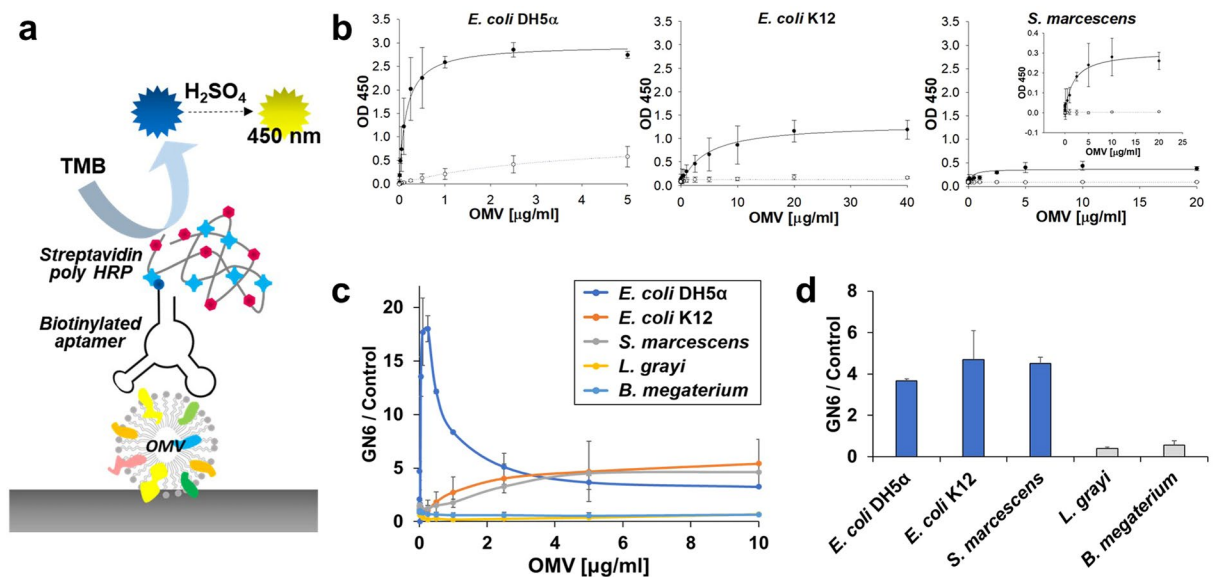


Figure 5. GN6-ELAA for Gram-negative bacterial OMVs. (a) Scheme of GN6 ELAA for bacterial OMVs. (b) Three Gram-negative bacterial OMVs showed highly sensitive binding to GN6 aptamer (●) rather than N40 control (○) at 250 nM concentration. (c) GN6 ELAA towards both Gram-negative and Gram-positive bacterial OMVs. (d) GN6 ELAA showed higher specificity to 5 μ g/mL of Gram-negative bacterial OMVs compared to 5 μ g/mL of Gram-positive bacterial OMVs from *L. grayi* and *B. megaterium*. Data represented mean \pm SD values of three independent experiments.

collected at 6,000 rpm for 5 min at 4 °C. The bound ssDNA was separated from bacterial cells by elution in Tris-EDTA buffer (50 mM Tris, pH 8.0, 10 mM EDTA, 1 mM MgCl₂, 5 mM KCl, 100 mM NaCl) at 95 °C for 5 min and cooled on ice for 5 min. The ssDNA after elution was collected at 13,000 rpm, 4 °C for 5 min, purified using PCI solution (Sigma Aldrich, USA), and precipitated in ethanol including 5 v/v% ammonium acetate and 1.5 v/v% glycogen. The PCR mixtures were made by ssDNA template (~20 ng), 0.4 μ M of forward and poly-A tailed reverse primer, MyTaq Reaction buffer, and 0.25 U My Taq DNA polymerase (Bioline, UK). After PCR, the reaction products were separated by 10% PAGE gel in 1X TBE (Tris-borate-EDTA). To separate the interested ssDNA, gel purifications in UREA-PAGE gel were performed using asymmetric poly-A tailed reverse primer. The dsDNA PCR product separated by forward primer in UREA gel was separated, heated at 65 °C for 30 min in elution buffer (10 mM Tris, pH 7.4, 1 mM EDTA, 750 mM NH₄OAc, 0.1% SDS) and collected in 0.3 M sodium acetate and 0.25 μ g/ μ L glycogen (pH 5.2). Subsequently, 2.5 volumes of 100% ethanol added and incubated at -80 °C for 12 h, followed by centrifugation at 13,000 rpm, 4 °C for 30 min. The DNA pellets were dissolved in water and quantified using BioSpecNano Spectrophotometer (SHIMADZU, Japan). For the next round of selection, 100 pmol of ssDNA from the first round was mixed with 10⁸ cells of *E. coli* K12. The following procedure was the same as above. Subsequently, ssDNA was isolated against *S. marcescens* and the same procedures were repeated four times (total 12 rounds). After the final round, the isolated ssDNA pools were amplified by RBC T&A cloning vector kit (Real Biotech, Taiwan). ssDNA aptamer candidates were transformed into competent *E. coli* DH5 α and then plasmid DNA were purified using QIAprep Spin Miniprep Kit (Qiagen Inc., Germany). The secondary structures were computationally predicted using M-fold algorithm (<http://mfold.rut.albany.edu>) at RT, [Na⁺] = 100 mM, and [Mg²⁺] = 5 mM.

Binding enrichment test using quantitative real-time PCR. The standard controls were made by serial dilution of samples. Each ssDNA sample was mixed with 0.2 μ M of forward, reverse 18-nt primers and SYBR® Premix Ex Taq™ (TliRNaseH Plus, Takara Bio Inc, Japan), followed by relative quantification analysis using StepOne™ Real-Time PCR System (Applied Biosystems®, USA) according to the manufacturer's protocol.

Fluorescence-based binding assays for aptamers. The binding affinity and capacity to bacteria were quantified by binding 3'-FAM labelled aptamers to the bacterial cells. For measuring the dissociation constants, 10⁸ cells of bacterial species were bound to different aptamer concentrations at RT for 15 min. To determine whether the aptamers showed non-specific binding to bacteria, the same concentrations of the negative controls as 3'-FAM labeled N40 library were incubated in the same bacteria used above. After incubation, the samples were washed three times in Tris buffer to remove unbound ssDNA, at 10,000 rpm, 4 °C for 10 min. Samples were resuspended in water, and their fluorescence intensity was measured using VICTOR X2 Multilabel Plate Reader (PerkinElmer, USA). The dissociation constant was measured by a non-linear regression fit model of SigmaPlot12.0. The binding efficiency or capacity of the two selected aptamers at 250 nM concentration was measured by incubating 10⁸ and 10⁵ cells of bacteria. It was also compared with that of 3'-FAM-labeled N40 random ssDNA upon incubation with 10⁸ and 10⁵ cells of bacteria.

Isolation and characterizations of OMVs. Bacterial cultures grown overnight in media were pelleted at 10,000 rpm for 30 min. The supernatant fraction was filtered through a 0.45 μm syringe (Merck Millipore, USA) to remove any remaining cell debris, and concentrated 50-fold by ultrafiltration using 100 kDa Amicon® Ultra-0.5 device (Merck Millipore). One more filtration was performed using 0.22 μm syringe filter (Merck Millipore). Next, OMVs were isolated by ultracentrifugation (Optima MAX-XP, Beckman Coulter, Inc., USA) at 150,000 rpm for 3 h at 4 °C, resuspended in PBS and stored at –80 °C. The protein concentrations were measured using micro BCA assay (Thermo Scientific, USA). To estimate the size distributions of the isolated OMVs, dynamic light scattering (DLS) was carried out using Zetasizer Nano ZS90 (Malvern, UK). Samples were diluted 1:1000 in PBS and processed at 25 °C under standard settings (Dispersant Refractive Index = 1.331, viscosity (cP) = 0.89). To visualize the binding between GN6 and *E. coli* DH5 α OMVs, 200 μg of streptavidin-coated magnetic beads (Dynabeads™ M-280 Streptavidin, Thermo Scientific, USA) and 50 pmol of GN6 aptamer were mixed for 30 min in mild shaking. After washing once, 10 $\mu\text{g}/\text{mL}$ of OMVs were added and incubated for 15 min, followed by washing several times to remove unbound OMVs. These samples were fixed in a 2% paraformaldehyde solution for 2 h and diluted in distilled water, followed by immobilization on the clean silicon chips under drying conditions. To make surface conductive, Au-Pd alloy was applied by sputtering before imaging. SEM using JSM-7100F was performed in 2 or 5 kV of beam energy.

Aptamer-based direct OMVs detection. For GN6 ELAA using bacterial OMVs, Nunc-Immuno 96 MicroWell solid plates (Thermo Scientific, USA) were used to immobilize bacterial OMVs in Tris buffer. After incubating OMVs at various concentrations in the plate overnight at 4 °C, the plate was washed twice and blocked using 2% BSA-Tris buffer for 2 h. After blocking, 20 pmol of GN6 aptamer and N40 control were separately added and incubated for 1 h. After washing 4 times, streptavidin-Poly HRP conjugate (Pierce, USA) was added and incubated for 30 min. After thoroughly washing 5 times in Tris buffer with 0.05% Tween-20, Ultra TMB-ELISA reagent (Thermo Scientific, USA) was added. After 15 min, 1 M sulfuric acid as stop solution was added. Absorbance at 450 nm was measured using Multiskan microplate photometer (Thermo Scientific, USA). The measured values were analyzed using non-linear regression fit model of SigmaPlot 12.0.

References

- Josenhans, C. & Suerbaum, S. The role of motility as a virulence factor in bacteria. *Int. J. Med. Microbiol.* **291**, 605–614 (2002).
- Delcour, A. H. Outer Membrane Permeability and Antibiotic Resistance. *Biochim. Biophys. Acta, Proteins Proteomics.* **1794**, 808–816 (2009).
- Rosenfeld, Y. & Shai, Y. Lipopolysaccharide (Endotoxin)-Host Defense Antibacterial Peptides Interactions: Role in Bacterial Resistance and Prevention of Sepsis. *Biochim. Biophys. Acta, Biomembr.* **1758**, 1513–1522 (2006).
- Beveridge, T. J. Structures of gram-negative cell walls and their derived membrane vesicles. *J. Bacteriol.* **181**, 4725–4733 (1999).
- Liu, Y., Defourny, K. A. Y., Smid, E. J. & Abee, T. Gram-Positive Bacterial Extracellular Vesicles and Their Impact on Health and Disease. *Front. Microbiol.* **9**, 1–8 (2018).
- Kulp, A. & Kuehn, M. J. Biological Functions and Biogenesis of Secreted Bacterial Outer Membrane Vesicles. *Annu. Rev. Microbiol.* **64**, 163–184 (2010).
- Ellis, T. N. & Kuehn, M. J. Virulence and Immunomodulatory Roles of Bacterial Outer Membrane Vesicles. *Microbiol. Mol. Biol. Rev.* **74**, 81–94 (2010).
- Voss, S., Fischer, R., Jung, G., Wiesmüller, K.-H. & Brock, R. A Fluorescence-Based Synthetic LPS Sensor. *J. Am. Chem. Soc.* **129**, 554–561 (2007).
- Mayall, R., Renaud-Young, M., Chan, N. & Birss, V. An Electrochemical Lipopolysaccharide Sensor Based on an Immobilized Toll-Like Receptor-4. *Biosens. Bioelectron.* **87**, 794–801 (2017).
- Hernout, O. *et al.* Design and Evaluation of Analogues of the Bacterial Cell-Wall Peptidoglycan Motif l-Lys-d-Ala-d-Ala for Use in a Vancomycin Biosensor. *Bioorg. Med. Chem. Lett.* **17**, 5758–5762 (2007).
- Zhang, F. *et al.* A Chiral Sensor Array for Peptidoglycan Biosynthesis Monitoring Based on MoS₂ Nanosheet-Supported Host-Guest Recognitions. *ACS Sens.* **3**, 304–312 (2018).
- Wang, Y., Ye, Z., Si, C. & Ying, Y. Monitoring of *Escherichia Coli* O157:H7 in Food Samples Using Lectin Based Surface Plasmon Resonance Biosensor. *Food. Chem.* **136**, 1303–1308 (2013).
- Xue, X., Pan, J., Xie, H., Wang, J. & Zhang, S. Fluorescence Detection of Total Count of *Escherichia Coli* and *Staphylococcus Aureus* on Water-Soluble CdSe Quantum Dots Coupled with Bacteria. *Talanta.* **77**, 1808–1813 (2009).
- Yang, M. *et al.* Highly Specific and Cost-Efficient Detection of *Salmonella Paratyphi A* Combining Aptamers with Single-Walled Carbon Nanotubes. *Sensors.* **13**, 6865–6881 (2013).
- Dudak, F. C. & Boyaci, I. H. Rapid and Label-Free Bacteria Detection by Surface Plasmon Resonance (SPR) Biosensors. *Biotechnol. J.* **4**, 1003–1011 (2009).
- Shen, Z. *et al.* Nonlabeled Quartz Crystal Microbalance Biosensor for Bacterial Detection Using Carbohydrate and Lectin Recognitions. *Anal. Chem.* **79**, 2312–2319 (2007).
- Lee, S.-H., Stubbs, D., Cairney, J. & Hunt, W. Rapid Detection of Bacterial Spores Using a Quartz Crystal Microbalance (QCM) Immunoassay. *IEEE Sens. J.* **5**, 737–743 (2005).
- Amiri, M., Bezaatpour, A., Jafari, H., Boukherroub, R. & Szunerits, S. Electrochemical Methodologies for the Detection of Pathogens. *ACS Sens.* **3**, 1069–1086 (2018).
- Ahmed, A., Rushworth, J. V., Hirst, N. A. & Millner, P. A. Biosensors for Whole-Cell Bacterial Detection. *Clin. Microbiol. Rev.* **27**, 631–646 (2014).
- Pathak, A. K., Creppage, K. E., Werner, J. R. & Cattadori, I. M. Immune Regulation of a Chronic Bacteria Infection and Consequences for Pathogen Transmission. *BMC Microbiol.* **10**, 1–9 (2010).
- Delios, M. M., Benagiano, M., Bella, C. D. & Amedei, A. T-Cell Response to Bacterial Agents. *J. Infect. Dev. Ctries.* **5**, 640–645 (2011).
- Ichzan, A. M. *et al.* Use of a Phosphatase-Like DT-Diaphorase Label for the Detection of Outer Membrane Vesicles. *Anal. Chem.* **91**, 4680–4686 (2019).
- Tuerk, C. & Gold, L. Systematic Evolution of Ligands by Exponential Enrichment: RNA Ligands to Bacteriophage T4 DNA Polymerase. *Science.* **249**, 505–510 (1990).
- Shangguan, D. *et al.* Aptamers Evolved from Live Cells as Effective Molecular Probes for Cancer Study. *Proc. Natl. Acad. Sci.* **103**, 11838–11843 (2006).
- Lavu, P. S. R., Mondal, B., Ramlal, S., Murali, H. S. & Batra, H. V. Selection and Characterization of Aptamers Using a Modified Whole Cell Bacterium SELEX for the Detection of *Salmonella Enterica* Serovar Typhimurium. *ACS Comb. Sci.* **18**, 292–301 (2016).

26. Hong, K. L. & Sooter, L. J. Single-Stranded DNA Aptamers against Pathogens and Toxins: Identification and Biosensing Applications. *Biomed. Res. Int.* **2015**, 1–31 (2015).
27. Artymiuk, P. J., Rice, D. W., Mitchell, E. M. & Willett, P. Structural Resemblance between the Families of Bacterial Signal-Transduction Proteins and of G Proteins Revealed by Graph Theoretical Techniques. *Protein Eng. Des. Sel.* **4**, 39–43 (1990).
28. Shortridge, M. D. & Powers, R. Structural and Functional Similarity between the Bacterial Type III Secretion System Needle Protein PrgI and the Eukaryotic Apoptosis Bcl-2 Proteins. *PLoS One.* **4**, 1–10 (2009).
29. Kim, Y. S., Song, M. Y., Jürging, J. & Kim, B. C. Isolation and Characterization of DNA Aptamers against *Escherichia Coli* Using a Bacterial Cell-Systematic Evolution of Ligands by Exponential Enrichment Approach. *Anal. Biochem.* **436**, 22–28 (2013).
30. White, R. *et al.* Generation of Species Cross-Reactive Aptamers Using “Toggle” SELEX. *Mol. Ther.* **4**, 567–573 (2001).
31. Dua, P. *et al.* Alkaline Phosphatase ALPPL-2 Is a Novel Pancreatic Carcinoma-Associated Protein. *Cancer Res.* **73**, 1934–1945 (2013).
32. Song, M. Y., Nguyen, D., Hong, S. W. & Kim, B. C. Broadly Reactive Aptamers Targeting Bacteria Belonging to Different Genera Using a Sequential Toggle Cell-SELEX. *Sci. Rep.* **7**, 1–10 (2017).
33. Lee, K. H. & Zeng, H. Aptamer-Based ELISA Assay for Highly Specific and Sensitive Detection of Zika NS1 Protein. *Anal. Chem.* **89**, 12743–12748 (2017).
34. Toh, S. Y., Citartan, M., Gopinath, S. C. & Tang, T.-H. Aptamers as a Replacement for Antibodies in Enzyme-Linked Immunosorbent Assay. *Biosens. Bioelectron.* **64**, 392–403 (2015).
35. Williams, K., Sobral, B. & Dickerman, A. A Robust Species Tree for The Alphaproteobacteria. *J. Bacteriol.* **189**, 4578–4586 (2007).
36. Pedersen, J. & Lindup, W. Interpretation and analysis of receptor binding experiments which yield non-linear Scatchard plots and binding constants dependent upon receptor concentration. *Biochem. Pharmacol.* **47**, 179–185 (1994).
37. Thoma, J. *et al.* Protein-enriched outer membrane vesicles as a native platform for outer membrane protein studies. *Commun. Biol.* **1**, 1–9 (2018).
38. McMahon, K. J., Castelli, M. E., Vescovi, E. G. & Feldman, M. F. Biogenesis of Outer Membrane Vesicles in *Serratia marcescens* Is Thermoregulated and Can Be Induced by Activation of the Rcs Phosphorelay System. *J. Bacteriol.* **194**, 3241–3249 (2012).
39. Shao, H. *et al.* Chip-Based Analysis of Exosomal mRNA Mediating Drug Resistance in Glioblastoma. *Nat. Commun.* **6**, 1–9 (2015).

Acknowledgements

This work was supported by the Agency for Defense Development through Chemical and Biological Detection Research Center.

Author Contributions

H.S.S. conducted experiment, analyzed experimental results, and wrote the manuscript. V.G. performed experiments and analyzed data. J.K.K. performed experiments and analyzed data. D.K.L. supervised experiments and wrote the manuscript. All authors reviewed the manuscript.

Additional Information

Supplementary information accompanies this paper at <https://doi.org/10.1038/s41598-019-49755-0>.

Competing Interests: D.K.L. is a founder and shareholder of OliX Pharmaceuticals.

Publisher’s note: Springer Nature remains neutral with regard to jurisdictional claims in published maps and institutional affiliations.



Open Access This article is licensed under a Creative Commons Attribution 4.0 International License, which permits use, sharing, adaptation, distribution and reproduction in any medium or format, as long as you give appropriate credit to the original author(s) and the source, provide a link to the Creative Commons license, and indicate if changes were made. The images or other third party material in this article are included in the article’s Creative Commons license, unless indicated otherwise in a credit line to the material. If material is not included in the article’s Creative Commons license and your intended use is not permitted by statutory regulation or exceeds the permitted use, you will need to obtain permission directly from the copyright holder. To view a copy of this license, visit <http://creativecommons.org/licenses/by/4.0/>.

© The Author(s) 2019